

THE ROLE OF FLOW VISUALIZATION
ON TRANSPORT PHENOMENA

Wen-Jei Yang

Department of Mechanical Engineering & Applied Mechanics
University of Michigan, Ann Arbor, Michigan 48109, U.S.A.

ABSTRACT Since Leonardo da Vinci advocated the experimental method during the Renaissance era, a gradual change took place from the purely philosophical science toward the observational (namely experimental) science of the present day. Various flow visualization techniques are introduced with their appropriate applications. Examples are presented to demonstrate how results obtained by flow visualization has been instrumental in discovering new flow phenomena which served as the basis in the development of natural laws, dimensionless parameters, or for the confirmation of concepts and theories.

1. Introduction

A natural phenomenon can be investigated by experimental methods, theoretical methods, or a combination of the two. The former can be classified into two kinds: flow measurement and visualization each with its own merit as well as shortcomings [1]. Results obtained by means of flow measurements are local at the point of a probe, but are quantitative. In contrast, the merit of flow visualization is global in nature but suffers from being qualitative. With the advent of digital computers and image processing techniques, the results of flow visualization today have higher quality and can be made in larger quantities [2]. Digital computers have made it possible to solve rather complex flow phenomena with results present in graphical form with the aid of computer graphics. This approach is named numerical flow visualization to distinguish it from experimental flow visualization that follows the conventional approach. A combination or hybrid of the two methods is obtained experimentally by solving the flow equations and appropriating initial and boundary conditions with some boundary conditions, which are difficult to define.

Recently, the divergence of this field, flow visualization, began based on the professional areas of applications: Medical vision refers to the application in medicine and surgery to aid in diagnosis and treatment [2], for example, computed tomography (CT), positron emission tomography (PET), nuclear magnetic resonance (NMR), or magnetic resonance imaging (MRI), just to name a few. Heat transfer visualization, which concentrates on applications in heat transfer field is just in its early stages. A brief history of flow visualization is available in Cheng [3].

This paper presents the role of flow visualization in transport phenomena. In general, transport phenomena refers to the transfer of physical properties such as materials, energy,

momentum, neutrons, electrons, and others. Here, only fluid flow phenomena are treated. Various flow visualization techniques are introduced. Historical events on the use of flow visualization are cited, which led to important flow phenomena. Contemporary applications are presented including both the experimental and numerical flow visualization techniques. Future trends are also predicted.

2. Methods Of Flow Visualization

The classification of flow visualization techniques may be somewhat different depending upon researchers. That listed in Table 1 is most common [1]. It classifies the techniques into four categories: wall tracing, tuft, tracer, and optical methods. Each group consists of a number of different sub-methods, depending on the manner of installation, substances, principles, etc. The wall tracing method enables the observation of certain flow characteristics close to a solid wall be it laminar, turbulent or separated flow pattern. This can be achieved by treating or coating the wall with a certain material: liquid film, sublimation, thermosensitive paint, electrolytic etching, and soluble chemical film. The tuft method is to attach one end of nylon or cotton yarn onto the wall. It includes the surface tuft for a shallow flow boundary layer and the depth tuft for a deeper one. The behavior of the tuft indicates flow characteristics to be laminar, turbulent, or separated flow. The characteristics of an external flow can be revealed by means of tuft grid consisting of a grid of wires attached with tufts. The grid is placed normal to the flow whose pattern is observed from downstream.

Table 1: Conventional flow visualization methods

Method	Type
Wall tracing	Liquid film Sublimation Thermosensitive paint Electrolytic etching Soluble chemical film
Tuft	Surface tuft Tuft grid Depth tuft
Tracer	Solid particles Liquids Gases
Chemical reaction	Chemical Electrolytic Photochemical
Electrical	Hydrogen bubble Spark Smoke wire
Optical	Shadowgraphy Schlieren Interferometry Holography Stereomicroscopy Moiré Liquid crystal

The tracer method is most suitable for the observation of whole flow field. It can be classified into direct injection, chemical reaction, and electrical methods. The direct injection method is historically the first means used in flow visualization, by addition of foreign materials into liquid or gas flow. It includes the release of dye, smoke, or solid particles into the fluid and the addition of bubbles into a gas stream. One can observe streamlines, streak lines, and path lines. The chemical method is to produce a tracer, typically a dye, by chemical, electrolytic, and photochemical methods. The electrical method is to produce gas bubbles as a tracer in a liquid flow, or to generate smoke and sparks in a gaseous flow.

Certain foreign agents are introduced into flow fields as a contrast medium in the above-mentioned flow visualization methods, assuming they do not affect the original flow. In the case of added particles, their motion is identical with that of the original flow. Another feature is that these flows are considered incompressible, i.e., the fluid has a uniform density throughout the flow field. However, in a compressible flow, the fluid density in the flow field may change spatially, or temporally, or both.

The optical method is non-invasive (i.e., no foreign additive) and utilizes density variation in the flow field for the observation of flow characteristics [4]. Figure 1 depicts the deflection and retardation of a light beam in a non-homogeneous refractive field. It is seen that the original beam OQ shifts to a new course (the disturbed beam) $O'Q'$ in the presence of a disturbance. It results in a change in the optical length, which can be determined by the integral $\int_0^s n ds$. Here, n denotes the index of refraction, which is equal to the square root of the dielectric constant for a gas. s is the arc length along the light path. There are three physical quantities of importance in Fig. 1:

- linear displacement QQ'
- angular displacement, $\theta - \theta'$
- phase shift between the disturbed and original beams, $\omega - \omega'$, due to their different optical path lengths.



Fig. 1 Deflection and retardation of a light ray in an optical disturbance.

All optical visualization methods are based on the recording of one of these three quantities or a combination of them. There are three basic methods corresponding to cases (i), (ii), and (iii). Case (i) is the shadowgraph, (ii) the schlieren method, and (iii) the Mach-Zehnder interferometry. Another distinction among the three methods is that (i) is sensitive to change in

the second derivative of density or n , (ii) to change in the density gradient, and (iii) measures absolute density changes.

Holography is the only method for accurately recording a three-dimensional image of a dynamic event. This is particularly useful in the observation of, for example, the droplet breakup and formation mechanisms, microscopic aspects of combustion and explosive events, and flow field around a supersonic projectile. Holography was invented in 1947 by D. Gabor. It is a mean for freezing all information contained in a light wave which can be reconstructed at a later time. The conventional photography records the information on only the amplitude pattern of a wave, i.e. two-dimensional projection of a three-dimensional flow scene. In wave and later reconstructs this wave with the aid of an appropriate visualization system to restore the original three-dimensional scenery. So, holographic flow visualization is a two-step procedure: first to freeze the flow scene holographically and later to reconstruct it with any of the conventional methods such as shadowgraph, schlieren, deflectometry, moiré, or interferometry. The choice of methods can be postponed. Many shadowgraphic systems obtain a schlieren photograph to produce a shadowgraph of the flow field with a schlieren system, or with a Wollaston prism to get schlieren interferometry. Holography has made some types of flow visualization possible that have not been achieved by other methods. Specifically, interferometry has been applied to compare two flow fields.

Liquid crystals can be painted or coated on a solid surface for measuring surface temperature or its changes, or boundary-layer flow visualization.

The advent of high-speed digital computers has led flow visualization methods into the second generation to observe flow characteristics both qualitatively as well as quantitatively. That is, the first generation implies the conventional, pure-experimental flow visualization methods since the inception by da Vinci. Recently, a new approach has prevailed, which is referred to as numerical flow visualization. The latter is obtained by numerically solving the flow equations, utilizing computer graphics to present the results in graphical form in color or black-and-white for easy viewing of the flow behavior. Results from the traditional flow visualization techniques can be enhanced in quality and digitized with the aid of image processing. Table 2 compares the first and second generation flow visualization method. The second generation method has found its extensive applications in medical visions, space exploration, and others.

Table 2: Flow visualization methods

First generation	Second generation
Traditional techniques	Computer-aided techniques
Qualitative information	Quantitative information
Contrast media for visualization	Recording, display, and storage for processing
Recording and display	Color as the parametric variable

3. The Role Of Flow Visualization

3.1. First Generation Techniques

The Renaissance marked a gradual change from the purely philosophical science toward the observational science of the present day. Leonardo da Vinci (1452-1519) was credited with

advocating the experimental approach as was noted by his statement "... as I have said, we must begin with experiment and try through it to discover the reason" [5]. He was the first to sketch the velocity distribution in a vortex, the formation of eddies at abrupt expansions and in wakes, and the profiles of free jets, as shown in Fig. 2. Thus, he is considered the first person to examine flow visualization. Using Fig. 3 for water flow in a river, da Vinci observed that "A river in each part of its length in an equal time gives passage to an equal quantity of water, whatever the width, the depth, the slope, the roughness, the tortuosity, ...". This is a statement on the principle of continuity, one of the fundamental laws in transport phenomena.



Fig. 2 Eddy formation in zones of separation.

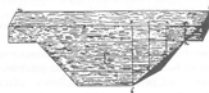


Fig. 3 Water flow in a river.

The Bernoulli's theorem marked the advent of hydrodynamics. Figure 4 shows typical Bernoulli efflux diagrams. D. Bernoulli (1700-1782) used the sketches to state the theorem: For any form of vessel and any velocity, the water pressure is always equal to $h_0 - h_v$. Here, h_0 designates the height corresponding to the velocity v , with which the water should emerge from a vertical opening after an infinite time with the vessel remaining full, and h_v is the height corresponding to the velocity of the water v , at a place and time for which one wishes to know the action. Note that the "live force" was already known to be proportional to the mass and the square of the velocity. It would yield the term presently known as kinetic energy with the introduction of the factor $1/2$. The Bernoulli's theorem represents the principle of conservation of energy, namely the first law of thermodynamics, under isothermal conditions.

Another example of diagrams describing the observation of flow is by B. Venturi (1746-1822). He demonstrated in Fig. 5 separation effects by means of various forms of mouth pieces fitted to the orifice: the effect of eddies formed at abrupt changes in section and the change in discharge which would result from their elimination.

The famous experiment of Reynolds (1842-1912) on flow patterns in a tube marked the dawn of contemporary flow visualization. A dye was injected into the flow as a tracer for the

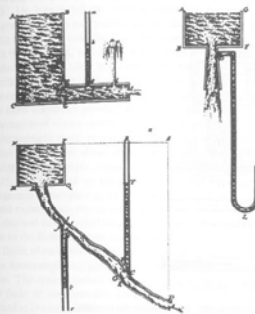


Fig. 4 Typical Bernoulli efflux diagrams.

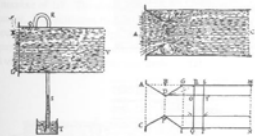


Fig. 5 Separation effects in mouthpieces.

observation of flow patterns. He demonstrated that the velocity, U , at which eddy motion began varies with the tube diameter, D , and the fluid properties (density, ρ , and dynamic viscosity, μ). It yielded a fairly constant value of this parameter, called Reynolds number defined as

$$Re = \frac{\rho U D}{\mu} \quad (1)$$

Reynold's sketches of the transitions from laminar to turbulent flow is depicted in Fig. 6.

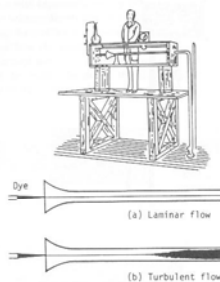


Fig. 6 Laminar and turbulent flows in pipe: (a) Laminar; (b) turbulent.

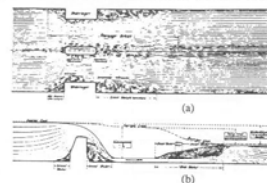


Fig. 7 Flow patterns (a) a local non-uniformity in plan due to a bridge pier and abutments, and (b) a local non-uniformity in profile at an overflow dam.

The success of constructing hydraulic structures was originated in model studies based largely on flow visualization in the early 20th century. It should be credited to both H. Engels (1854-1945) and T. Rehbock (1864-1950). Figure 7 shows flow patterns constructed from laboratory (model) observations of (a) a local non-uniformity in plan due to a bridge pier and abutments, and (b) a local non-uniformity in profile at an overflow dam.

It is generally agreed that the founder of present-day fluid mechanics is L. Prandtl (1875-1953). He introduced the concept, called the theory of the boundary layer, which have presaged essentially every aspect of boundary layer analysis and control. The concept states that the study of a particular flow phenomenon can be divided into two interdependent parts: One is the free fluid, which can be treated as inviscid according to the vorticity principles of Helmholtz, and the other is the transition layers at the fixed boundaries whose movement is controlled by the free fluid, yet which in turn, give the free movement its characteristic stamp by the emission of vortex streets. Figure 8 depicts a schematic of flow visualization apparatus, which used aluminum powders as the tracer to demonstrate boundary-layer phenomena, i.e., the formation of vortex streets in the region of separation behind a cylinder. Figure 9 presents two photographs made in a demonstration flume illustrating (a) the normal wake behind a cylinder and (b) the effect of removing the boundary through a slot on the upper side (boundary-layer control). Prandtl's development of the mixing length theory in turbulent flow in 1925 was inspired by his flow visualization experiment. Later, he photographed the development of turbulent spots for flow along a flat plate. After the observation of Hiemenz's repeated experiments on cross flow around a cylinder in a water tunnel, T. von Karman (1881-1963) derived an analytical solution for the eddy formation behind cylindrical bodies in 1911, known as the Karman vortex streets. By the turn of the 20th century, the continued divergence of the fields of endeavor in fluid mechanics had brought them very far apart. It is in this period that the increasingly stringent demands of aeronautics gave rise to an effectively new branch of science. The optical method of visualizing procedures had contributed greatly to advancement in the field of compressible flows [4]. The simplest arrangement is the shadowgraph, attributed to Dvorak (1880). It uses no optical equipment except a spherical mirror or a lens to make the light parallel. Because of its simplicity, the shadowgraph is useful for a quick survey of the flow pattern, especially shock-wave geometry, in addition to turbulence and boundary-layer measurements. Figure 10 is a shadowgraph of a sphere in free flight through air at a Mach number of 1.7. The shock wave is seen to induce turbulent separation downstream from the equator. The schlieren method developed by Foucault (1859) and Toepler (1864), has a knife-edge as its only principal component. Because of relative simplicity in the optical arrangement combined with a high degree of resolution, it has been most frequently applied optical visualization system in aerodynamics.

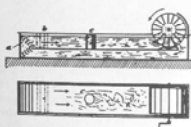


Fig. 8 Flume with hand-operated paddle wheel used by Prandtl to demonstrate boundary-layer phenomena.



Fig. 9 Photographs made in demonstration flume : (a) normal wake behind a cylinder; (b) effect of removing boundary layer through slot on upper side.

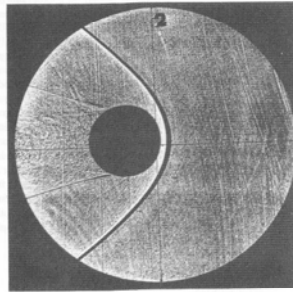


Fig. 10 Shadowgraph of a sphere flying at a Mach number of $M=1.7$.

The first person to use the schlieren method for supersonic flow visualization was E. Mach [6]. Figure 11 depicts a schlieren photograph of a brass bullet in a supersonic flight through air, exhibiting the bow (or bend) shock wave. Later (in 1893), he obtained quantitative measurements of the strength of the shock wave using the Mach-Zehnder interferometer developed by L. Mach (his son).

The hydrogen bubble method was employed to investigate the turbulent boundary layer on a flat plate, revealing the coherent structure in the viscous sublayer.

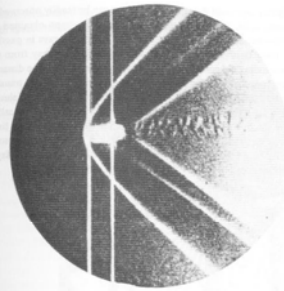


Fig. 11 Brass bullet in supersonic flight through air [6].

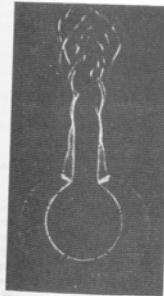


Fig. 12 Visualization of the boundary layer and film heat-transfer coefficient around a horizontal tube in free-convection flow by a schlieren photograph [7].

The dimensions of the boundary layer and the temperature field can be readily observed in schlieren or interference photographs. Figure 12 is a schlieren photograph obtained by Schmidt in 1932 for natural convection on a horizontal cylinder. The light rays in passing through the heated boundary layer (with a density gradient) were deflected away from the cylinder, and the dark zone surrounding the contour indicates the boundary layer. The distance of the heart-shaped bright line from the cylinder contour is proportional to the heat transfer coefficient. A similar natural convection phenomena was photographed using a Mach-Zehnder interferometer, as shown in Fig. 13. One observes a field of dark and bright bands (called interference fringes) around the shadow of the cylinder. The dark interference bands are lines of constant air density or equivalent isotherms, under the assumption of constant pressure. The temperature gradient in the air along the surface and consequently the boundary layer thickness and heat transfer coefficient can be determined from the schlieren photograph.

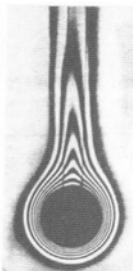
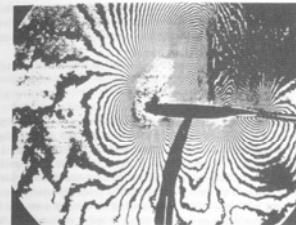


Fig. 13 Isotherms around a horizontal tube in free-convection flow as revealed by an interference photograph [8].

Holography [9, 10] is unique in that a wavefront modulated by only the optical system can be subtracted from one that has both optical system and flow field modulation, removing the effects of the optics. Effects of a steady part of a flow field can be subtracted, leaving an unsteady component, which might otherwise be overshadowed by the steady part. Figure 14-a depicts a flow field with a weak unsteady component being overshadowed by a strong steady part. The unsteady flow is clearly seen in Fig. 14-b only after subtracting off the steady flow effects. It reveals the vortex street in the model wake, the unsteady shock wave, and the free

stream turbulence. In addition, one can zoom in on specific portions of the flow field with high spatial resolution (not shown), leaving other parts of the flow field out.



(a)



(b)

Fig. 14 Potential flow field (a) overshadowed by a strong steady flow; (b) holographically subtracted leaving unsteady field.

Holographic flow visualization played an important role in providing quantitative results for the development and evaluation of theoretical models and computer codes for shock wave / boundary layer interaction. A progress was made to extend a real time holographic flow visualization. For example, a real time holographic interferogram of a transonic channel flow was obtained showing the density and pressure distribution.

Three-dimensional flows can be obtained from tomographic solutions provided that enough interferograms are made at the correct viewing angles through the flow. The flow in cascades, inside combustion engines, inside compressor fans, and in other confined regions presents the problems of timing and optical access.

The reader may refer to the proceedings of a series of international symposia on flow visualization (for example, [11, 12, 13, 14, 15, 16]).

3.2. Second Generation Techniques [2]

Recent scientific development have made radical improvements in the versatility and quality of flow visualization. These include: (1) power lasers, capable of dynamically illuminating complex unsteady flows, especially in a pulsed mode with computer-controlled scanning; (2) high-transmissivity fiber optics that provide optical access to realistic configuration beyond the reach of mirror systems; and (3) digital image processing that extracts information not visible to the eye and presents results in the form most suitable for productive use by the scientists and engineers. The second half of the 20th century marked the dawn of a new era for computer-assisted flow visualization motivated by the needs in space exploration followed by the domestic applications in medicine. Computer graphics is employed to display, either in colors or contours, a large amount of data generated by computer simulations (called numerical flow visualization), medical imaging systems, experiments (conventional flow visualization), satellites, and other high-volume data sources.

One of the main objectives in flow visualization has been to quantize the observed flow phenomena through digital image processing. In contrast, a new technique is emerging to achieve the reverse. That is, to produce the image of flow phenomena from computer generated data using color graphic techniques. This method can be used to reconstruct the experimental flow field from limited data flow to give a more physical meaning to the information. The technique allows a numerical (computer) experiment to be visualized much like a physical one, thus hastening interpretation.

The advent of computer-generated graphics opens a new era in the field of flow visualization. The traditional means of flow visualization is through the use of "hardware". Flow visualization by computer-generated color graphics can be classified into four categories:

- (i) Computer-generated graphic display of flow solutions
- (ii) Computer-aided display of flow field survey data
- (iii) Computer-assisted flow visualization (CAV) techniques
- (iv) Combined computation and measurement

With the cost of PCs falling and the computational capacity of PCs rising, more and more flow visualization studies will be computer assisted. The most important applications of CAV are found in aerodynamics and combustion, three-dimensional flow, turbulent boundary layers, medical imaging technology, and environments.

In aerodynamic applications, computational fluid dynamics (CFD) is changing the relative roles of experiment and computation in the engineering of aircraft and aerospace vehicles. Numerical flow visualization resulting from CFD incorporated with computer graphics has recently achieved its prominence, spearheaded by the efforts of NASA's research centers. This is especially true in hypersonic flows. Turbulent boundary layer is a primary object of flow visualization and image processing. Due to three-dimensionality and time-dependency of such flows, a real-time, multi-view visualization technique is needed to facilitate the viewing of change of three-dimensional structures. Likewise, combustion phenomena need a similar treatment.

Fluid flow phenomena occur typically in the vascular, pulmonary and lymphatic system in the human body where transfer of heat, mass, and electricity take place. The difference in body-scanning systems has led to six distinct medical vision methods: computed tomography (CT); digital subtraction angiography (DSA); nuclear magnetic resonance (NMR), also called magnetic resonance imaging (MRI); radioisotope imaging (RII); sonography (SONO), and thermography (TT). The information obtained by each of these image acquisition devices is computer-processed (called image processing) and the results are displayed. Figure 15 presents machine vision in medicine, which is the marriage of imaging devices to computers. The medical vision has found a great use, like a miracle, in morphography and diagnostics. The basic discovery of nuclear magnetic resonance in 1946 and the development of CT scanners in 1972 marked two great strides in medicine since the discovery of the x ray by W.C. Roentgen in 1895 which has been developed as a seeing machine. Both were honored by the Nobel Prize.

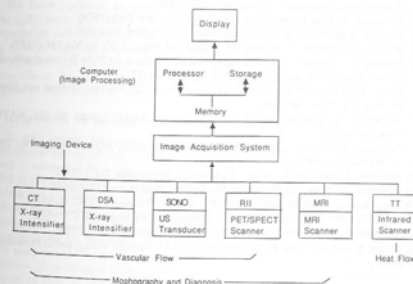


Fig. 15 Machine vision in medicine: the marriage of imaging devices and a computer.

4. Summary

All natural laws are derived empirically. Experimental techniques in transport processes are classified into flow visualization and measurement. This paper has presented the role of flow visualization in the derivation of natural laws and important phenomena in heat and fluid flow since the Renaissance era. In the second half of the 20th century, the advent of high-speed computing machines brought a revolutionary change in the role of flow visualization to include the quantization of information in flow fields being observed through experimental means or numerical computations. Both computer graphics and image processing aid in display and in quality enhancement.

Flow visualization has been instrumental in the advancement of medical vision for diagnostics and treatments, space exploration, and high-tech industries. It will continue to serve as the vanguard for the exploration of new flow phenomena and as a vital instrument in the study of complex phenomena such as three-dimensional flow, turbulence, combustion, medical imaging, and more.

5. References

- [1] Yang, Wen-Jei (ed.), Handbook of Flow Visualization, Hemisphere, Washington, D.C. (1989).
- [2] Yang, Wen-Jei, Computer Aided Flow Visualization, Second Generation Techniques, CRC Press Boca Raton, Florida (1994).
- [3] Cheng, K.C., "Internal Flows", Chapter 27 in Handbook of Flow Visualization (Wen-Jei Yang, editor), Hemisphere, Washington, D.C. (1989).
- [4] Merzkirch, W., Flow Visualization, Academic Press, New York (1974).
- [5] Rouse, H. and Ince, S., History of Hydraulics, Dover, New York (1957).
- [6] Mach, E. and Salcher, P., Sitzungsber. Wien Akad. Wiss. II '95, pp.764-780 (1887).
- [7] Schmidt, E., "Schlieren aufnahmen des Temperaturfeldes in der Nahe Wärmeabgebender Körper", Forsch. Geb. Ingenieurwes., Vol.3, pp. 81-89 (1932).
- [8] Eckert, E.R.G. and Drake, R.M., Jr., Introduction to the Transfer of Heat and Mass, McGraw-Hill, New York (1950).
- [9] Merzkirch, W., Techniques of Flow Visualization, AGARDograph No.302, NATO, Germany (1987).
- [10] Trolinger, J.D., Laser Applications in Flow Diagnostics, AGARDograph No. 296, NATO, Belgium (1988).
- [11] Asanuma, T., Flow Visualization I, Hemisphere, Washington, D.C. (1978).
- [12] Merzkirch, W., Flow Visualization II, Hemisphere, Washington, D.C. (1982).
- [13] Yang, Wen-Jei, Flow Visualization III, Hemisphere, Washington, D.C. (1985).
- [14] Veret, C., 1987, Flow Visualization IV, Hemisphere, Washington, D.C. (1987).
- [15] Reznicek, R., Flow Visualization V, Hemisphere, Washington D.C. (1990).
- [16] Tanida, Y. and Miyashiro, H., Flow Visualization VI, Springer Verlag, Berlin-Heidelberg (1992).

THE SIXTH ASIAN CONGRESS OF FLUID MECHANICS May 22-26, 1995, Singapore

THE ROLE OF FLUID MECHANICS IN ENHANCING COASTAL ENVIRONMENTAL QUALITIES

Theodore Yaotsu Wu
Engineering Science, California Institute of Technology
Pasadena, CA 91125, U.S.A.

The physical and geophysical processes taking place in coastal waters involving fluid mechanics of transport of mass, momentum and energy in various forms are very complex in manifest. Of these phenomena spanning over a wide scope, this paper selects three specific classes of problems to illustrate the roles that fluid mechanics can play in helping improve our knowledge and technology for maintaining and enhancing our coastal environmental qualities. These problems are:

- (1) interaction between long gravity waves on coastal waters and beach;
- (2) terminal effects of internal waves in coastal waters; and
- (3) interaction between bidirectional nonlinear dispersive waves.

For these problems, an appropriate theoretical model is the generalized Boussinesq (gB) model (Wu, Ref [1]) which is known to be reliable in predicting generation, propagation and evolution of long gravity waves in coastal water of depth slowly varying in both longshore and seaward directions. It is based on the premise that both the nonlinear and dispersive effects are weak but nevertheless on a par with the net linear effects. For the above three problems, solutions will be presented using various degrees of modification of the gB model.

1. Long waves on straight beach of variable slope; longshore currents

To gain insight into coastal dynamics in nature, we first consider the three-dimensional run-up of long waves on a straight beach of variable downward slope which is connected to an open ocean of uniform depth. A linear long-wave theory, which is the linearized version of the gB model, is applied to obtain the fundamental solution for a uniform train of sinusoidal waves obliquely incident upon the beach, without wave breaking. The solution, obtained in terms of a series of rapid convergence (Zhang & Wu, Ref [2]), is characterized by two parameters, one being the incidence angle (β , the angle subtended by the incoming wave vector and the landward axis) and the wave number (κ) scaled by the beach width. For waves at normal incidence ($\beta = 0$) on a sloping plane beach, the runup given by the linear theory is equal to that by nonlinear theory. At oblique incidences, the run-up is found to increase with increasing incidence angle up to about $\beta = 45^\circ$. For waves at nearly grazing incidences, $85^\circ < \beta < 90^\circ$, run-up is significant only for the waves in a set of eigenmodes being trapped within the beach at resonance with the exterior ocean waves (see figure 1). The impact of this trapped grazing waves upon coastal environmental quality is not yet in focus, but its effects should be of interest on coastal